

Prime editing optimized RTT permits the correction of the c.8713C>T mutation in *DMD* gene

Cedric Happi Mbakam,^{1,2} Joel Rousseau,^{1,2} Yaoyao Lu,^{1,2} Anne Bigot,³ Kamel Mamchaoui,³ Vincent Mouly,³ and Jacques P. Tremblay^{1,2}

¹CHU de Québec Research Centre, Laval University, Québec, QC G1V 0A6, Canada; ²Molecular Medicine Department, Faculty of Medicine, Laval University, Québec, QC G1V 4G2, Canada; ³Myology Research Center, Institute of Myology, 75013 Paris, France

Duchenne muscular dystrophy is a severe debilitating genetic disease caused by different mutations in the *DMD* gene leading to the absence of dystrophin protein under the sarcolemma. We used CRISPR-Cas9 prime editing technology for correction of the c.8713C>T mutation in the *DMD* gene and tested different variations of reverse transcription template (RTT) sequences. We increased by 3.8-fold the editing percentage of the target nucleotide located at +13. A modification of the protospacer adjacent motif sequence (located at +6) and a silent mutation (located at +9) were also simultaneously added to the target sequence modification. We observed significant differences in editing efficiency in interconversion of different nucleotides and the distance between the target, the nicking site, and the additional mutations. We achieved 22% modifications in myoblasts of a *DMD* patient, which led to dystrophin expression detected by western blot in the myotubes that they formed. RTT optimization permitted us to improve the prime editing of a point mutation located at +13 nucleotides from the nick site to restore dystrophin protein.

INTRODUCTION

Duchenne muscular dystrophy (DMD) is a lethal X-linked disease characterized by progressive muscle wasting with high burden on patients and family members.^{1–4} The prevalence is estimated to 19.8 per 100,000 live male births, 7.1 cases per 100,000 males, and 2.8 cases per 100,000 individuals in the general population.⁵ The prevalence is also evaluated at 10.9, 6.1, 2.2, and 1.9 per 100,000 males respectively in France, Canada, the United Kingdom, and the United states.⁴ The disease is caused by mutations in the *DMD* gene coding for the dystrophin protein, which is normally located under the sarcolemma.^{6,7} Different types of mutations leading to DMD have been identified in the *DMD* gene, which is one of the biggest human genes,⁸ and different therapeutic strategies have been developed.^{9,10} These mutations include exonic and intronic duplications accounting for 10%–15% of DMD mutations, small insertions and deletions (3%), point mutations (nonsense and missense mutations, splice site mutations, and mid intronic mutations, 26%) and single- or multi-exon deletions (60%–70%).^{7,11} Many research groups have been using CRISPR-Cas9

genome editing to modify the *DMD* gene to restore the dystrophin expression.^{12–19} The CRISPR-Cas9 technology uses a specific single guide RNA (sgRNA) to target and cut DNA at a desired site to induce different types of modifications following DNA repair by non-homologous end-joining or homology-directed repair (HDR).²⁰ HDR-mediated DMD correction has been shown in a canine model of DMD to be associated with a set of challenges affecting the editing efficiency.²¹ The recent CRISPR-Cas9 prime editing technique is more precise and permits base-to-base conversion, replacement, and insertion and deletion in the genome.^{22–26} For prime editing, the SpCas9 (*Streptococcus pyogenes*) nuclease has been modified into an SpCas9 nickase (SpCas9n) and is fused with an engineered reverse transcriptase from *Murine leukemia virus*. Prime editing also required a modified sgRNA called prime editing guide RNA (pegRNA).²² Prime editing has already been used to correct *DMD* gene mutations located close to the SpCas9n nick site.^{14,19,27} However, the efficacy of prime editing decays rapidly when the target nucleotide is far from the nick site. Our study aimed to improve the prime editing effectiveness for the correction of c.8713C>T point mutation in exon 59 of the *DMD* gene, which is positioned far from the nick site, i.e., at +13 from the nick site.

RESULTS

Verifying whether prime editing permits a specific modification at +13 from the nick site

We initially verified whether prime editing could induce a nucleotide mutation in exon 59 of *DMD* gene to change a stop codon (TGA) at position 8,713 into an arginine codon (CGA) to restore the dystrophin protein expression. Since at the beginning of the project we did not have myoblasts containing that mutation, we initially decided to induce a c.8713C>T mutation to create a stop codon instead of inducing the correction of the mutation. The cytidine (C) nucleotide of CGA codon coding for an arginine amino acid (R) had to be

Received 22 February 2022; accepted 28 September 2022;
<https://doi.org/10.1016/j.omtn.2022.09.022>

Correspondence: Jacques P. Tremblay, CHU de Québec Research Centre, Laval University, Québec, QC G1V 0A6, Canada.

E-mail: jacques-p.tremblay@crchul.ulaval.ca



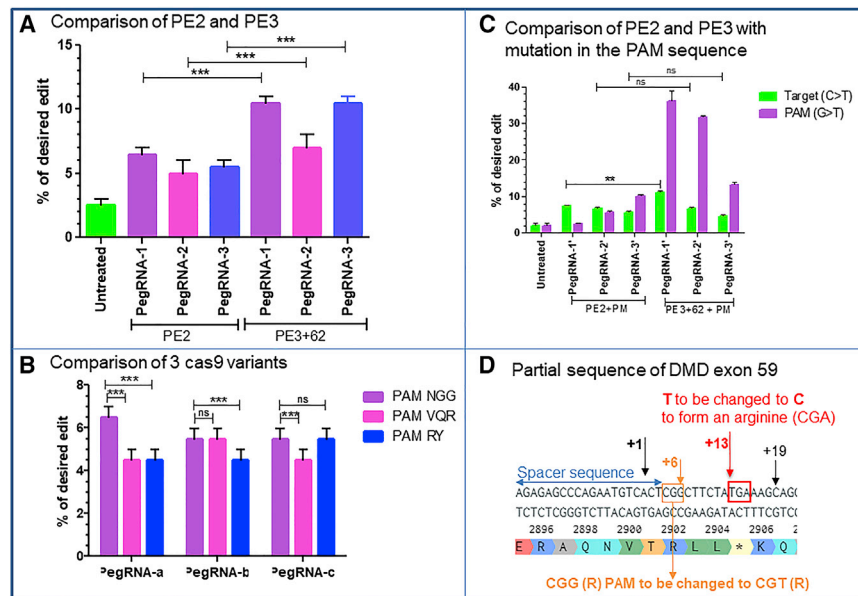


Figure 1. PE2 and PE3 editing of DMD exon 59 using SpCas9 and variants

(A) Editing efficiency using the initial three pegRNAs for the PE2 and PE3 strategies (using an sgRNA inducing a nick at position +62) to induce c.8713C>T mutation in exon 59 of *DMD* gene. The differences between pegRNA1, pegRNA2, and pegRNA3 for PE2 and PE3 were statistically significant ($***p < 0.001$). (B) Results obtained with three different pegRNAs (a, b, and c) designed individually for each nuclease variant recognizing the NGG PAM (for SpCas9), the NGAN PAM (for SpCas9-VQR), and the NNN PAM (for SpCas9-RY). ns indicates that the differences between the pegRNAs of these Cas9 variants were not significant. The asterisks indicate that the differences were statistically significant ($***p < 0.001$). (C) Editing efficiency for PE2 and PE3 strategies using three pegRNAs containing two mutations each: the target mutation and the mutation in the PAM sequence (PM). The difference of mutation at the target site was significant only for pegRNA1 used for PE2 and PE3. (D) Partial sequence of *DMD* exon 59 carrying a nonsense mutation to be corrected (TGA sequence shown by the red square at the position +13). The red square is the TGA stop codon to be corrected to a CGA

codon which is an arginine (R). The orange square contains the sequence of the PAM CGG to be modified to CGT to increase the editing efficiency of the nonsense mutation at the position +13. The numbers +1 and +13 represent different positions from the nick site, and the blue arrow is the 20-nt spacer sequence. These experiments were done in independent triplicates ($n = 3$). The non-parametric Mann-Whitney U test was performed to calculate the p values.

changed into a thymine (T) nucleotide to form the TGA stop codon located at the position +13 from the closest SpCas9 possible nick site (Figure 1D). This is considered to be a little too far from the nick site and thus at a less efficient position for the nucleotide modification.²² We designed three pegRNA sequences (Table 1, rows 1A) named pegRNA1 (RTT16, PBS14), pegRNA2 (RTT15, PBS12), and pegRNA3 (RTT15, PBS16) for the rapid screening of targeted nucleotide modification. For the PE2-NGG strategy,²² the HEK293T cells were co-transfected with pCMV-PE2 plasmid (Addgene #132775) coding for the normal SpCas9n (using an NGG protospacer adjacent motif [PAM]) fused with the reverse transcriptase and pU6-pegRNA-GG-acceptor plasmid (Addgene #132777) coding for one of the pegRNA constructs. Three days after the transfection, a part of exon 59 of *DMD* gene was PCR amplified from harvested cells using a pair of primers (Table 2) and Sanger sequenced. The results indicated that the editing percentages were $6.5\% \pm 0.7\%$, $5\% \pm 1.4\%$, and $5.5\% \pm 0.7\%$ for pegRNA1, pegRNA2, and pegRNA3, respectively (Figure 1A). For the PE3 strategy,²² we inserted an additional sgRNA to the pBSU6 plasmid to induce a second nick at position +62 from the initial nick site by the pegRNA. We co-transfected HEK293T cells with the pCMV-PE2 plasmid, the pU6-pegRNA-GG-acceptor plasmid, and the pBSU6 plasmid. The results showed $10.5\% \pm 0.7\%$, $7\% \pm 1.4\%$, and $10.5\% \pm 0.7\%$ editing percentage, respectively for pegRNA1, pegRNA2, and pegRNA3 (Figure 1A).

The use of SpCas9 variants to induce the same target nucleotide modification

Since the +13 position was less favorable for prime editing because it is far from the nick site, we decided to test other SpCas9n variants,

which used a PAM closer to the target nucleotide than when using the normal NGG SpCas9 PAM. We thus constructed two plasmid variants, the SpCas9n-VQR recognizing an NGAN PAM²⁸ and the SpCas9n-RY recognizing the NNN PAM sequence (N being any nucleotide)²⁹ to make, respectively, the PE2-VQR and the PE2-SpRY.³⁰ The PE2-VQR was making it possible to induce the same nucleotide modification at +1 instead of at +13 with NGG PAM, and the PE2-RY was permitting us to make the modification at +3 considering the combination of nucleotide in PAM sequence that showed better results in other studies.^{29,30} We designed three other pegRNAs for each of these two variants, namely pegRNAa, pegRNAb, and pegRNAc, with different reverse transcription template (RTT), primer binding site (PBS), and spacer sequences (Table 1, rows 1B). The codified pegRNAa, pegRNAb, and pegRNAc for PE2-NGG variant correspond to the same sequences described in Table 1 (rows 1A). The PE2-NGG, PE2-VQR, and PE2-SpRY variants were each co-transfected with one of the appropriate pegRNA plasmids in HEK293T cells. Three days after transfection the cells were harvested, and a partial DNA sequence of exon 59 was PCR amplified and Sanger sequenced. The results showed editing percentages of up to $6.5\% \pm 0.7\%$, $5.5\% \pm 0.5\%$, and $5.5\% \pm 0.7\%$, respectively with PE2-NGG, PE2-VQR, and PE2-RY (Figure 1B). Thus, PE2-NGG remained the best editing method although the target nucleotide was at +13 from the nick site.

Modification of the PAM to increase the edit of the target nucleotide

Since the editing percentages were only around 6%, we hypothesized that changing the second G nucleotide of the SpCas9n CGG PAM,

Table 1. pegRNA sequences

Names	Spacer sequences	PBS sequences	RTT sequences	sgRNA for PE3
Initial experiments in HEK293T (1A)				
pegRNA1	GAGAGAGCCCAGAATGTCACT	GACATTCTGGGCTC	TTCATAGAAGCCGAGT	GTCTGCCAGTCAGCGGAGTGC
pegRNA2	GAGAGAGCCCAGAATGTCACT	GACATTCTGGGC	TCATAGAAGCCGAGT	GTCTGCCAGTCAGCGGAGTGC
pegRNA3	GAGAGAGCCCAGAATGTCACT	GACATTCTGGGCTCTC	TCATAGAAGCCGAGT	GTCTGCCAGTCAGCGGAGTGC
Cas9 variants experiments in HEK293T (1B)				
pegRNAa-VQR	GAGAATGTCACTCGGCTTCTA	AAGCCGAGTG	CCTGCTTTCATAG	GTCTGCCAGTCAGCGGAGTGC
pegRNAb-VQR	GAGAATGTCACTCGGCTTCTA	AAGCCGAGTGACA	CCTGCTTTCATAG	GTCTGCCAGTCAGCGGAGTGC
pegRNAc-VQR	GAGAATGTCACTCGGCTTCTA	AAGCCGAGTGACATTC	CCTGCTTTCATAG	GTCTGCCAGTCAGCGGAGTGC
pegRNAa-RY	GATGTCACTCGGCTTCTACGA	TAGAAGCCGAGTGA	AGCCTGCTTCA	GCCTAAAACCTTGTCATATTG
pegRNAb-RY	GATGTCACTCGGCTTCTACGA	TAGAAGCCGAGTGACA	TCAGCCTGCTTCA	GCCTAAAACCTTGTCATATTG
pegRNAc-RY	GATGTCACTCGGCTTCTACGA	TAGAAGCCGAGTGAC	TCCTCAGCCTGCTTCA	GCCTAAAACCTTGTCATATTG
PAM modification experiments in HEK293T (1C)				
pegRNA1'(16-14)	GAGAGAGCCCAGAATGTCACT	GACATTCTGGGCTC	TTCATAGAAGaCGAGT	GTCTGCCAGTCAGCGGAGTGC
pegRNA2'(15-12)	GAGAGAGCCCAGAATGTCACT	GACATTCTGGGC	TCATAGAAGaCGAGT	GTCTGCCAGTCAGCGGAGTGC
pegRNA3'(15-16)	GAGAGAGCCCAGAATGTCACT	GACATTCTGGGCTCTC	TCATAGAAGaCGAGT	GTCTGCCAGTCAGCGGAGTGC
Nucleotide position from the PAM experiments in HEK293T (1D)				
+13C>T	GAGAGAGCCCAGAATGTCACT	GACATTCTGGGCTC	TTCATAGAAGaCGAGT	GTCTGCCAGTCAGCGGAGTGC
+12A>T	GAGAGAGCCCAGAATGTCACT	GACATTCTGGGCTC	TTCGAAGAAGaCGAGT	GTCTGCCAGTCAGCGGAGTGC
+11T>A	GAGAGAGCCCAGAATGTCACT	GACATTCTGGGCTC	TTCGTGAAGaCGAGT	GTCTGCCAGTCAGCGGAGTGC
+10C>T	GAGAGAGCCCAGAATGTCACT	GACATTCTGGGCTC	TTCGTAAAAGaCGAGT	GTCTGCCAGTCAGCGGAGTGC
+9T>A	GAGAGAGCCCAGAATGTCACT	GACATTCTGGGCTC	TTCGTAGTAGaCGAGT	GTCTGCCAGTCAGCGGAGTGC
+8T>A	GAGAGAGCCCAGAATGTCACT	GACATTCTGGGCTC	TTCGTAGATGaCGAGT	GTCTGCCAGTCAGCGGAGTGC
+7C>T	GAGAGAGCCCAGAATGTCACT	GACATTCTGGGCTC	TTCGTAGAAaCGAGT	GTCTGCCAGTCAGCGGAGTGC
+5G>T	GAGAGAGCCCAGAATGTCACT	GACATTCTGGGCTC	TTCGTAGAAGaAGAGT	GTCTGCCAGTCAGCGGAGTGC
+4C>T	GAGAGAGCCCAGAATGTCACT	GACATTCTGGGCTC	TTCGTAGAAGaCAAGT	GTCTGCCAGTCAGCGGAGTGC
+3T>A	GAGAGAGCCCAGAATGTCACT	GACATTCTGGGCTC	TTCGTAGAAGaCGTGT	GTCTGCCAGTCAGCGGAGTGC
+2C>T	GAGAGAGCCCAGAATGTCACT	GACATTCTGGGCTC	TTCGTAGAAGaCGAAT	GTCTGCCAGTCAGCGGAGTGC
+1A>T	GAGAGAGCCCAGAATGTCACT	GACATTCTGGGCTC	TTCGTAGAAGaCGAGA	GTCTGCCAGTCAGCGGAGTGC
Other nucleotides than PAM experiments in HEK293T (1E)				
+1A>T	GAGAGAGCCCAGAATGTCACT	GACATTCTGGGCTC	TTCATAGAAGCCGAGa	GTCTGCCAGTCAGCGGAGTGC
+2C>T	GAGAGAGCCCAGAATGTCACT	GACATTCTGGGCTC	TTCATAGAAGCCGAaT	GTCTGCCAGTCAGCGGAGTGC
+3T>A	GAGAGAGCCCAGAATGTCACT	GACATTCTGGGCTC	TTCATAGAAGCCGtGT	GTCTGCCAGTCAGCGGAGTGC
+4C>T	GAGAGAGCCCAGAATGTCACT	GACATTCTGGGCTC	TTCATAGAAGCCaAGT	GTCTGCCAGTCAGCGGAGTGC
+5G>T	GAGAGAGCCCAGAATGTCACT	GACATTCTGGGCTC	TTCATAGAAGCaGAGT	GTCTGCCAGTCAGCGGAGTGC
+6G>T	GAGAGAGCCCAGAATGTCACT	GACATTCTGGGCTC	TTCATAGAAGaCGAGT	GTCTGCCAGTCAGCGGAGTGC
+7C>T	GAGAGAGCCCAGAATGTCACT	GACATTCTGGGCTC	TTCATAGAaCCGAGT	GTCTGCCAGTCAGCGGAGTGC
+8T>A	GAGAGAGCCCAGAATGTCACT	GACATTCTGGGCTC	TTCATAGAtGCCGAGT	GTCTGCCAGTCAGCGGAGTGC
+9T>A	GAGAGAGCCCAGAATGTCACT	GACATTCTGGGCTC	TTCATAGtAGCCGAGT	GTCTGCCAGTCAGCGGAGTGC
+10C>T	GAGAGAGCCCAGAATGTCACT	GACATTCTGGGCTC	TTCATaAaAGCCGAGT	GTCTGCCAGTCAGCGGAGTGC
+11T>A	GAGAGAGCCCAGAATGTCACT	GACATTCTGGGCTC	TTCATtGAAGCCGAGT	GTCTGCCAGTCAGCGGAGTGC
+12A>T	GAGAGAGCCCAGAATGTCACT	GACATTCTGGGCTC	TTCaAaAGAAGCCGAGT	GTCTGCCAGTCAGCGGAGTGC
+14G>T	GAGAGAGCCCAGAATGTCACT	GACATTCTGGGCTC	TtAaTAGAAGCCGAGT	GTCTGCCAGTCAGCGGAGTGC
+15A>T	GAGAGAGCCCAGAATGTCACT	GACATTCTGGGCTC	TaCaTAGAAGCCGAGT	GTCTGCCAGTCAGCGGAGTGC
+16A>T	GAGAGAGCCCAGAATGTCACT	GACATTCTGGGCTC	ATCaTAGAAGCCGAGT	GTCTGCCAGTCAGCGGAGTGC

(Continued on next page)

Table 1. Continued

Names	Spacer sequences	PBS sequences	RTT sequences	sgRNA for PE3
+17A>T	GAGAGAGCCCAGAATGTCACT	GACATTCTGGGCTC	GCaTTCATAGAAGCCGAGT	GTCTGCCAGTCAGCGGAGTGC
+18G>T	GAGAGAGCCCAGAATGTCACT	GACATTCTGGGCTC	GaTTCATAGAAGCCGAGT	GTCTGCCAGTCAGCGGAGTGC
+19C>T	GAGAGAGCCCAGAATGTCACT	GACATTCTGGGCTC	aCTTCATAGAAGCCGAGT	GTCTGCCAGTCAGCGGAGTGC
Type of nucleotide in PAM experiments in HEK293T (1F)				
+6G>A	GAGAGAGCCCAGAATGTCACT	GACATTCTGGGCTC	TTCATAGAAGtCGAGT	GTCTGCCAGTCAGCGGAGTGC
+6G>C	GAGAGAGCCCAGAATGTCACT	GACATTCTGGGCTC	TTCATAGAAGgCGAGT	GTCTGCCAGTCAGCGGAGTGC
RTT length modification experiments in HEK293T (1G)				
RTT13	GAGAGAGCCCAGAATGTCACT	GACATTCTGGGCTC	ATAGAAGCCGAGTGACATTCTGGGCTC	GTCTGCCAGTCAGCGGAGTGC
RTT15	GAGAGAGCCCAGAATGTCACT	GACATTCTGGGCTC	TCGTAGAAGCCGAGTGACATTCTGGGCTC	GTCTGCCAGTCAGCGGAGTGC
RTT16	GAGAGAGCCCAGAATGTCACT	GACATTCTGGGCTC	TTCATAGAAGCCGAGTGACATTCTGGGCTC	GTCTGCCAGTCAGCGGAGTGC
RTT18	GAGAGAGCCCAGAATGTCACT	GACATTCTGGGCTC	CTTTCGTAGAAGCCGAGTGACATTCTGGGCTC	GTCTGCCAGTCAGCGGAGTGC
RTT19	GAGAGAGCCCAGAATGTCACT	GACATTCTGGGCTC	GCTTTCATAGAAGCCGAGTGACATTCTGGGCTC	GTCTGCCAGTCAGCGGAGTGC
RTT21	GAGAGAGCCCAGAATGTCACT	GACATTCTGGGCTC	CTGCTTTCGTAGAAGCCGAGTGACATTCTGGGCTC	GTCTGCCAGTCAGCGGAGTGC
RTT22	GAGAGAGCCCAGAATGTCACT	GACATTCTGGGCTC	CCTGCTTTCATAGAAGCCGAGTGACATTCTGGGCTC	GTCTGCCAGTCAGCGGAGTGC
RTT24	GAGAGAGCCCAGAATGTCACT	GACATTCTGGGCTC	AGCCTGCTTTCGTAGAAGCCGAGTGACATTCTGGGCTC	GTCTGCCAGTCAGCGGAGTGC
RTT25	GAGAGAGCCCAGAATGTCACT	GACATTCTGGGCTC	CAGCCTGCTTTCATAGAAGCCGAGTGACATTCTGGGCTC	GTCTGCCAGTCAGCGGAGTGC
RTT28	GAGAGAGCCCAGAATGTCACT	GACATTCTGGGCTC	CCTCAGCCTGCTTTCATAGAAGCCGAGTGACATTCTGGGCTC	GTCTGCCAGTCAGCGGAGTGC
RTT31	GAGAGAGCCCAGAATGTCACT	GACATTCTGGGCTC	CCTCCTCAGCCTGCTTTCATAGAAGCCGAGTGACATTCTGGGCTC	GTCTGCCAGTCAGCGGAGTGC
RTT35	GAGAGAGCCCAGAATGTCACT	GACATTCTGGGCTC	TTGACCTCCTCAGCCTGCTTTCATAGAAGCCGAGTGACATTCTGGGCTC	GTCTGCCAGTCAGCGGAGTGC
RTT39	GAGAGAGCCCAGAATGTCACT	GACATTCTGGGCTC	AGTATTGACCTCCTCAGCCTGCTTTCATAGAAGCCGAGTGACATTCTGGGCTC	GTCTGCCAGTCAGCGGAGTGC
RTT42	GAGAGAGCCCAGAATGTCACT	GACATTCTGGGCTC	ACTCAGTATTGACCTCCTCAGCCTGCTTTCATAGAAGCCGAGTGACATTCTGGGCTC	GTCTGCCAGTCAGCGGAGTGC
RTT length and PAM modification experiments in HEK293T (1H)				
RTT13	GAGAGAGCCCAGAATGTCACT	GACATTCTGGGCTC	ATAGAAGaCGAGTGACATTCTGGGCTC	GTCTGCCAGTCAGCGGAGTGC
RTT15	GAGAGAGCCCAGAATGTCACT	GACATTCTGGGCTC	TCGTAGAAGaCGAGTGACATTCTGGGCTC	GTCTGCCAGTCAGCGGAGTGC
RTT16	GAGAGAGCCCAGAATGTCACT	GACATTCTGGGCTC	TTCATAGAAGaCGAGTGACATTCTGGGCTC	GTCTGCCAGTCAGCGGAGTGC
RTT18	GAGAGAGCCCAGAATGTCACT	GACATTCTGGGCTC	CTTTCGTAGAAGaCGAGTGACATTCTGGGCTC	GTCTGCCAGTCAGCGGAGTGC
RTT19	GAGAGAGCCCAGAATGTCACT	GACATTCTGGGCTC	GCTTTCATAGAAGaCGAGTGACATTCTGGGCTC	GTCTGCCAGTCAGCGGAGTGC

(Continued on next page)

Table 1. Continued

Names	Spacer sequences	PBS sequences	RTT sequences	sgRNA for PE3
RTT21	GAGAGAGCCCAGAATGTCACT	GACATTCTGGGCTC	CTGCTTTCGTAGAAGaCG AGTGACATTCTGGGCTC	GTCTGCCAGTCAGCGGAGTGC
RTT22	GAGAGAGCCCAGAATGTCACT	GACATTCTGGGCTC	CCTGCTTTCATAGAAGaC GAGTGACATTCTGGGCTC	GTCTGCCAGTCAGCGGAGTGC
RTT24	GAGAGAGCCCAGAATGTCACT	GACATTCTGGGCTC	AGCCTGCTTTCGTAGAAGaC CGAGTGACATTCTGGGCTC	GTCTGCCAGTCAGCGGAGTGC
RTT25	GAGAGAGCCCAGAATGTCACT	GACATTCTGGGCTC	CAGCCTGCTTTCATAGAA GaCGAGTGACATTCT GGGCTC	GTCTGCCAGTCAGCGGAGTGC
RTT28	GAGAGAGCCCAGAATGTCACT	GACATTCTGGGCTC	CCTCAGCCTGCTTTCATA GAAGaCGAGTGACATTCT TGGGCTC	GTCTGCCAGTCAGCGGAGTGC
RTT31	GAGAGAGCCCAGAATGTCACT	GACATTCTGGGCTC	CCTCCTCAGCCTGCTTTC ATAGAAGaCGAGTGACA TCTGGGCTC	GTCTGCCAGTCAGCGGAGTGC
RTT35	GAGAGAGCCCAGAATGTCACT	GACATTCTGGGCTC	TTGACCTCCTCAGCCTG CTTTCATAGAAGaCGAG TGACATTCTGGGCTC	GTCTGCCAGTCAGCGGAGTGC
RTT39	GAGAGAGCCCAGAATGTCACT	GACATTCTGGGCTC	AGTATTGACCTCCTCAG CCTGCTTTCATAGAAGaC GAGTGACATTCTGGGCTC	GTCTGCCAGTCAGCGGAGTGC
RTT42	GAGAGAGCCCAGAATGTCACT	GACATTCTGGGCTC	ACTCAGTATTGACCTCCTC AGCCTGCTTTCATAGAAG aCGAGTGACATTCTGGGCTC	GTCTGCCAGTCAGCGGAGTGC
RTT length, PAM, and additional nucleotide modification experiments in HEK293T (II)				
+1A>G	GAGAGAGCCCAGAATGTCACT	GACATTCTGGGCTC	GCTTTCATAGAAGaCGAGC	GTCTGCCAGTCAGCGGAGTGC
+2C>T	GAGAGAGCCCAGAATGTCACT	GACATTCTGGGCTC	GCTTTCATAGAAGaCGAAT	GTCTGCCAGTCAGCGGAGTGC
+3C>T	GAGAGAGCCCAGAATGTCACT	GACATTCTGGGCTC	GCTTTCATAGAAGaCGgGT	GTCTGCCAGTCAGCGGAGTGC
+4C>T	GAGAGAGCCCAGAATGTCACT	GACATTCTGGGCTC	GCTTTCATAGAAGaCAAGT	GTCTGCCAGTCAGCGGAGTGC
+5G>A	GAGAGAGCCCAGAATGTCACT	GACATTCTGGGCTC	GCTTTCATAGAAGaTGAGT	GTCTGCCAGTCAGCGGAGTGC
+7C>T	GAGAGAGCCCAGAATGTCACT	GACATTCTGGGCTC	GCTTTCATAGAAaCGAGT	GTCTGCCAGTCAGCGGAGTGC
+8T>C	GAGAGAGCCCAGAATGTCACT	GACATTCTGGGCTC	GCTTTCATAGAGGaCGAGT	GTCTGCCAGTCAGCGGAGTGC
+9T>C	GAGAGAGCCCAGAATGTCACT	GACATTCTGGGCTC	GCTTTCATAGgAGaCGAGT	GTCTGCCAGTCAGCGGAGTGC
+10C>T	GAGAGAGCCCAGAATGTCACT	GACATTCTGGGCTC	GCTTTCATAAAAGaCGAGT	GTCTGCCAGTCAGCGGAGTGC
+11T>C	GAGAGAGCCCAGAATGTCACT	GACATTCTGGGCTC	GCTTTCATGGAAGaCGAGT	GTCTGCCAGTCAGCGGAGTGC
+12A>G	GAGAGAGCCCAGAATGTCACT	GACATTCTGGGCTC	GCTTTCaCaGAAGaCGAGT	GTCTGCCAGTCAGCGGAGTGC
+14G>A	GAGAGAGCCCAGAATGTCACT	GACATTCTGGGCTC	GCTTTTATAGAAGaCGAGT	GTCTGCCAGTCAGCGGAGTGC
+15A>G	GAGAGAGCCCAGAATGTCACT	GACATTCTGGGCTC	GCTTcATAGAAGaCGAGT	GTCTGCCAGTCAGCGGAGTGC
+16A>G	GAGAGAGCCCAGAATGTCACT	GACATTCTGGGCTC	GCTCTCATAGAAGaCGAGT	GTCTGCCAGTCAGCGGAGTGC
+17A>G	GAGAGAGCCCAGAATGTCACT	GACATTCTGGGCTC	GCCTTCATAGAAGaCGAGT	GTCTGCCAGTCAGCGGAGTGC
+18G>A	GAGAGAGCCCAGAATGTCACT	GACATTCTGGGCTC	GTTTTcATAGAAGaCGAGT	GTCTGCCAGTCAGCGGAGTGC
+19C>T	GAGAGAGCCCAGAATGTCACT	GACATTCTGGGCTC	ACTTTCATAGAAGaCGAGT	GTCTGCCAGTCAGCGGAGTGC
+3T>C	GAGAGAGCCCAGAATGTCACT	GACATTCTGGGCTC	CCTCCTCAGCCTGCTTTC ATAGAAGaCGgGT	GTCTGCCAGTCAGCGGAGTGC
+9T>C	GAGAGAGCCCAGAATGTCACT	GACATTCTGGGCTC	CCTCCTCAGCCTGCTTTC ATAGgAGaCGgGT	GTCTGCCAGTCAGCGGAGTGC
+12A>G	GAGAGAGCCCAGAATGTCACT	GACATTCTGGGCTC	CCTCCTCAGCCTGCTTTC CAcAGAAAGaCGgGT	GTCTGCCAGTCAGCGGAGTGC
+15A>G	GAGAGAGCCCAGAATGTCACT	GACATTCTGGGCTC	CCTCCTCAGCCTGCTTcC ATAGAAGaCGgGT	GTCTGCCAGTCAGCGGAGTGC

(Continued on next page)

Table 1. Continued

Names	Spacer sequences	PBS sequences	RTT sequences	sgRNA for PE3
Five simultaneous mutations in HEK293T experiments (1J)				
ADD MUT	GAGAGAGCCCAGAATGTCACT	GACATTCTGGGCTC	GCATTCAAAGaCGAAT	GTCTGCCAGTCAGCGGAGTGC
Type of nucleotides at the target and in additional mutation in HEK293T experiments (1K)				
+13C>T	GAGAGAGCCCAGAATGTCACT	GACATTCTGGGCTC	TTCATAGAAGaCGAGT	GTCTGCCAGTCAGCGGAGTGC
+13C>G	GAGAGAGCCCAGAATGTCACT	GACATTCTGGGCTC	TTCCTAGAAGaCGAGT	GTCTGCCAGTCAGCGGAGTGC
+13C>A	GAGAGAGCCCAGAATGTCACT	GACATTCTGGGCTC	TTCTTAGAAGaCGAGT	GTCTGCCAGTCAGCGGAGTGC
+13C>T	GAGAGAGCCCAGAATGTCACT	GACATTCTGGGCTC	CCTCCTCAGCCTGCTT TCATAGAAGaCGAGT	GTCTGCCAGTCAGCGGAGTGC
+13C>G	GAGAGAGCCCAGAATGTCACT	GACATTCTGGGCTC	CCTCCTCAGCCTGCTT TCCTAGAAGaCGAGT	GTCTGCCAGTCAGCGGAGTGC
+13C>A	GAGAGAGCCCAGAATGTCACT	GACATTCTGGGCTC	CCTCCTCAGCCTGCTT TCTTAGAAGaCGAGT	GTCTGCCAGTCAGCGGAGTGC
T +3T>C	GAGAGAGCCCAGAATGTCACT	GACATTCTGGGCTC	GCTTTCATAGAAGaCGgGT	GTCTGCCAGTCAGCGGAGTGC
T +3T>G	GAGAGAGCCCAGAATGTCACT	GACATTCTGGGCTC	GCTTTCATAGAAGaCGcGT	GTCTGCCAGTCAGCGGAGTGC
T +3T>A	GAGAGAGCCCAGAATGTCACT	GACATTCTGGGCTC	GCTTTCATAGAAGaCGtGT	GTCTGCCAGTCAGCGGAGTGC
G +3T>C	GAGAGAGCCCAGAATGTCACT	GACATTCTGGGCTC	GCTTTCCTAGAAGaCGgGT	GTCTGCCAGTCAGCGGAGTGC
G +3T>G	GAGAGAGCCCAGAATGTCACT	GACATTCTGGGCTC	GCTTTCCTAGAAGaCGcGT	GTCTGCCAGTCAGCGGAGTGC
G +3T>A	GAGAGAGCCCAGAATGTCACT	GACATTCTGGGCTC	GCTTTCCTAGAAGaCGtGT	GTCTGCCAGTCAGCGGAGTGC
A +3T>C	GAGAGAGCCCAGAATGTCACT	GACATTCTGGGCTC	GCTTTCCTAGAAGaCGgGT	GTCTGCCAGTCAGCGGAGTGC
A +3T>G	GAGAGAGCCCAGAATGTCACT	GACATTCTGGGCTC	GCTTTCCTAGAAGaCGcGT	GTCTGCCAGTCAGCGGAGTGC
A +3T>A	GAGAGAGCCCAGAATGTCACT	GACATTCTGGGCTC	GCTTTCCTAGAAGaCGtGT	GTCTGCCAGTCAGCGGAGTGC
T +3T>C	GAGAGAGCCCAGAATGTCACT	GACATTCTGGGCTC	CCTCCTCAGCCTGCTTT CATAGAAGaCGgGT	GTCTGCCAGTCAGCGGAGTGC
T +3T>G	GAGAGAGCCCAGAATGTCACT	GACATTCTGGGCTC	CCTCCTCAGCCTGCTTT CATAGAAGaCGcGT	GTCTGCCAGTCAGCGGAGTGC
T +3T>A	GAGAGAGCCCAGAATGTCACT	GACATTCTGGGCTC	CCTCCTCAGCCTGCTTT CATAGAAGaCGtGT	GTCTGCCAGTCAGCGGAGTGC
G +3T>C	GAGAGAGCCCAGAATGTCACT	GACATTCTGGGCTC	CCTCCTCAGCCTGCTTT CcTAGAAGaCGgGT	GTCTGCCAGTCAGCGGAGTGC
G +3T>G	GAGAGAGCCCAGAATGTCACT	GACATTCTGGGCTC	CCTCCTCAGCCTGCTTT CcTAGAAGaCGcGT	GTCTGCCAGTCAGCGGAGTGC
G +3T>A	GAGAGAGCCCAGAATGTCACT	GACATTCTGGGCTC	CCTCCTCAGCCTGCTTT CcTAGAAGaCGtGT	GTCTGCCAGTCAGCGGAGTGC
A +3T>C	GAGAGAGCCCAGAATGTCACT	GACATTCTGGGCTC	CCTCCTCAGCCTGCTTT CtTAGAAGaCGgGT	GTCTGCCAGTCAGCGGAGTGC
A +3T>G	GAGAGAGCCCAGAATGTCACT	GACATTCTGGGCTC	CCTCCTCAGCCTGCTTT CtTAGAAGaCGcGT	GTCTGCCAGTCAGCGGAGTGC
A +3T>A	GAGAGAGCCCAGAATGTCACT	GACATTCTGGGCTC	CCTCCTCAGCCTGCTTT CtTAGAAGaCGtGT	GTCTGCCAGTCAGCGGAGTGC
Myoblast correction (1L)				
+3T>C	GAGAGAGCCCAGAATGTCACT	GACATTCTGGGCTC	GCTTTCGTAGAAGaCGgGT	GTCTGCCAGTCAGCGGAGTGC
+9T>C	GAGAGAGCCCAGAATGTCACT	GACATTCTGGGCTC	GCTTTCGTAGgAGaCGAGT	GTCTGCCAGTCAGCGGAGTGC
+12A>G	GAGAGAGCCCAGAATGTCACT	GACATTCTGGGCTC	GCTTTCGcAGAAGaCGAGT	GTCTGCCAGTCAGCGGAGTGC
+15A>G	GAGAGAGCCCAGAATGTCACT	GACATTCTGGGCTC	GCTTTCGtTAGAAGaCGAGT	GTCTGCCAGTCAGCGGAGTGC
+3T>C	GAGAGAGCCCAGAATGTCACT	GACATTCTGGGCTC	CCTCCTCAGCCTGCTTTC GTAGAAGaCGgGT	GTCTGCCAGTCAGCGGAGTGC

(Continued on next page)

Table 1. Continued

Names	Spacer sequences	PBS sequences	RTT sequences	sgRNA for PE3
+9 T>C	GAGAGAGCCCAGAATGTCACT	GACATTCTGGGCTC	CCTCCTCAGCCTGCTTTC GTAG G AGaCGgGT	GTCTGCCAGTCAGCGGAGTGC
+12A>G	GAGAGAGCCCAGAATGTCACT	GACATTCTGGGCTC	CCTCCTCAGCCTGCTTT CG a AGAGaCGgGT	GTCTGCCAGTCAGCGGAGTGC
+15A>G	GAGAGAGCCCAGAATGTCACT	GACATTCTGGGCTC	CCTCCTCAGCCTGCTT cCGTAGAAGaCGAGT	GTCTGCCAGTCAGCGGAGTGC

Nucleotides in boldface represent the modifications to induce using the primer binding site (PBS) and reverse transcriptase template (RTT).

which is an arginine codon, into a T nucleotide to form the CGT codon, which remains an arginine codon, could improve the editing efficiency by preventing the DNA to be nicked again by SpCas9n after a previous successful modification. We designed three new pegRNAs (pegRNA1', pegRNA2', and pegRNA3') (Table 1, rows 1C) containing both the intended nucleotide modification at +13 and an additional PAM modification at +6. The results showed editing percentages of $7.3\% \pm 0.5\%$, $6.5\% \pm 0.7\%$, and $5.5\% \pm 0.7\%$ for the PE2 strategy, which represented 1.2-fold increase for pegRNA1' and pegRNA2' compared with the pegRNAs not mutating the PAM (Figure 1C). We also used an additional sgRNA to nick at +62 for the PE3 strategy leading to $11\% \pm 1\%$, $6.5\% \pm 0.7\%$, and $4.5\% \pm 0.7\%$ editing percentage, which represented a 1.4-fold increase only for the pegRNA1' (Figure 1C). The results also highlighted a high editing percentage of $36\% \pm 4.2\%$ for the G nucleotide of the CGG PAM to be changed into T nucleotide (Figure 1C). This confirmed that the frequency of nucleotide editing is very high for nucleotides located near the nick site.

Checking whether the position of the intended mutation is influenced by the modification induced in the PAM sequence

To verify whether the intended nucleotide modification efficiency is influenced by the PAM modification and the distance from the PAM or from the nick site, we decided to modify each nucleotide individually from +1 to +13 while maintaining the PAM edit at position +6 (Figure 2A). We used the pegRNA1', which was the best among the three pegRNAs, and the sgRNA to induce a second nick at +62. We designed 12 other pegRNAs (Table 1, rows 1D) from the pegRNA1' to induce at the position +1 the modification of A to T (+1A>T), +2C>T, +3T>A, +4C>T, +5G>T, +7C>T,

+8T>A, +9T>A, +10C>T, +11T>A, +12A>T, and +13C>T but always maintaining +6G>T in the PAM sequence. The highest editing rate was observed with +1A>T that showed $59.3\% \pm 3.7\%$ and $69\% \pm 4.3\%$ modification, respectively for the intended modification (+1A>T) and the PAM modification (+6G>T) (Figure 2A). We observed that the efficiency varies depending on the type of nucleotide to be changed, the distance from the nicking site, and the modification of the PAM sequence. These results also confirmed that the editing efficiency decreased progressively for nucleotides to be changed from positions +11 to +13.

Checking whether the modification of nucleotides other than the PAM could influence the nucleotide mutation at +13

From the same pegRNA1', we designed 18 other pegRNAs (Table 1, rows 1E) to modify each nucleotide from position +1 to +19 while maintaining the intended edit at +13 to verify whether the modification of nucleotides other than the PAM sequence (+6G>T) could influence our intended modification at +13 using the PE3 strategy (Figure 2B). The results showed $21\% \pm 1.4\%$ of desired modification at +13 when a G was changed to A simultaneously at position +19 (Figure 2B). This percentage was on average 2-fold higher than the results obtained by modifying simultaneously only the PAM sequence. These results confirmed that the editing efficiency at the target (+13C>T) is influenced by the modification of other nucleotides around it. Unfortunately, none of the second mutations introduced around the desired modification with the highest efficiency at +13 could mediate a silent mutation. Thus, our best option remained the PAM modification that can mediate a silent mutation of the arginine (R) codon.

Verifying the influence of the type of nucleotide to change in the PAM sequence

To answer the question as to whether the type of nucleotide change in the PAM sequence can have more or less influence on the desired modification at +13, we designed different pegRNAs (Table 1, rows 1F) to check the combination of different nucleotides at position +6 in the PAM sequence while maintaining the desired +13C>T mutation. The different possible combinations were G>T, G>A, and G>C. The PE3 results showed average editing percentages of $10.5\% \pm 0.7\%$, $7.5\% \pm 0.7\%$, and $8\% \pm 1.4\%$, respectively for C>T modification at +13 and $37.5\% \pm 2.1\%$, $27.5\% \pm 4.1\%$, and $33\% \pm 2.8\%$, respectively for the G>T, G>A, and G>C modifications in the PAM sequence (Figure 3).

Table 2. Primer sequences for PCR and sequencing

Primer names	Sequences
Pr PCR Fwd	GCACTCTTATCTCAATGAGAGG
Pr PCR Rev	AGGTGATCTTGAGAGAGTC
Pr Sanger sequencing	ATCACCTCAGCTGGCGCAGCT
Pr deep sequencing Fwd	ACACTGACGACATGGTTCTACA CGTTAATCAGTAGGTTACCCCTC
Pr deep sequencing Rev	TACGGTAGCAGAGACTTGGTCT TTGAGGTCCAGCTCATCCGT

Sequences in boldface represent specific barcode sequences for deep sequencing.

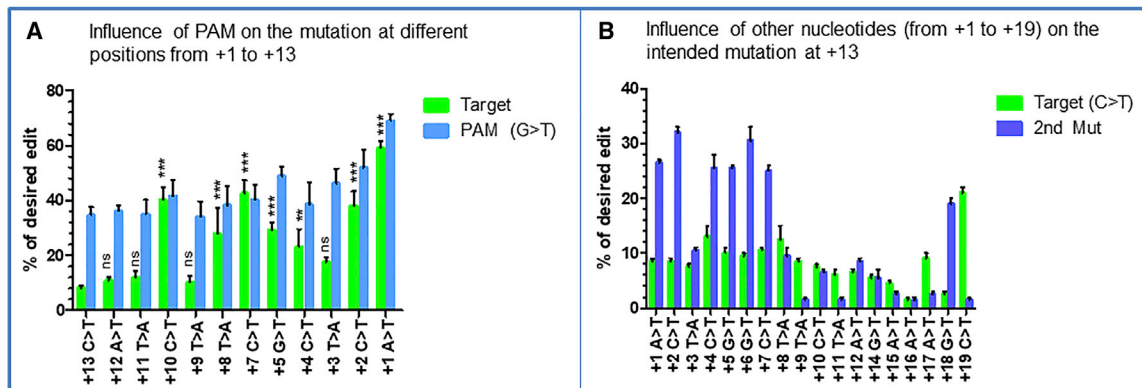


Figure 2. Influence of the PAM nucleotide or other nucleotides in the target

(A) Results obtained when the guanine nucleotide at +6 from the PAM is modified into a thymine simultaneously with the modification of one nucleotide located at positions spanning +1 to +13 from the nick induced by the SpCas9n. Position +13 is indicated in the red square in Figure 1D. At this position 13, the CGA codon is to be changed to a TGA codon. (B) Results obtained when modifications are done from +1 to +19 while modifying simultaneously the target nucleotide at +13. These experiments were done in independent triplicates ($n = 3$). All the editing percentages at different targets were compared with the modification at +13. The p values were calculated using the non-parametric Mann-Whitney U test. *** $p < 0.001$; ** $p = 0.01$; ns, non-significant difference.

Modification of RTT length to influence the edit at +13

To verify whether modification of the RTT length could increase the results of the modifications at +13, we designed ten pegRNAs from the initial pegRNA1 (RTT16, PBS14) with RTT length varying from 13 (RTT13) to 42 (RTT42) (Table 1, rows 1G). The PE2 strategy results showed an increased in editing efficiency up to $13.5\% \pm 2.1\%$ for RTT25 (Figure 4A). The PE3 results with the same sgRNA at +62 showed up to $18.5\% \pm 0.7\%$ modification (Figure 4B). We also designed ten other RTT sequences carrying both the modification in the PAM sequence at position +6 and at the target at +13 (Table 1, rows 1H). The PE2 results indicated up to $13\% \pm 2.8\%$ modification at the target with the best RTT length ranging from RTT25 to RTT35

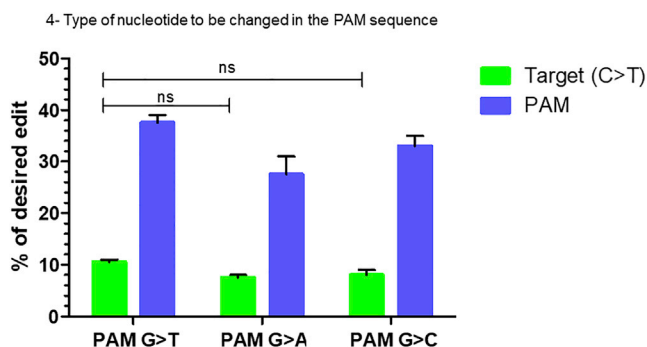


Figure 3. The type of nucleotide to be changed at the target

This figure shows the difference in editing efficiency to induce c.8713C>T mutation in exon 59 of *DMD* gene while also changing one nucleotide of the PAM sequence. The PAM sequence CGG is changed respectively to CGT, CGA, and CGC, which are all coding for the arginine amino acid. Each of these modifications was done simultaneously with the modification of the target at +13 changing C to T. These experiments were done in independent triplicates ($n = 3$). The differences in editing efficiency at the target for the different modifications in PAM sequences were not statistically significant (ns).

(Figure 4C). The PE3 results showed a pick of $20.5\% \pm 0.7\%$ modification at the target nucleotide (+13C>T) for RTT31 (Figure 4D), which was 7% higher than the pick observed with the PE3 strategy without modification in the PAM (Figure 4C). From these observations, we reasoned that the RTT variation and an additional mutation could have an influence in the editing efficiency at the target.

Additional mutations in the RTT sequence

To check whether additional mutation in the RTT sequence could increase the target modification at +13, we designed 19 new pegRNA sequences from the initial pegRNA1 (Table 1, rows 1I). Each pegRNA contained three mutations always including the target mutation at +13, the mutation in the PAM, and with only the third additional mutation changing at different positions spanning from +1 to +19. Among the 19 designed pegRNAs, four had the RTT31 because it exhibited the highest editing percentage in previous results. For the four pegRNAs with RTT31, the third mutation was selected to induce a silent mutation respectively at positions +3 changing a T to C (+3T>C RTT31), +9 changing a T to C (+9T>C RTT31), +12 changing an A to G (+12A>G RTT31), and +15 changing an A to G (+15A>G RTT31). On the other hand, the 15 remaining pegRNAs contained RTT19 with the third mutation spanning from +1 to +19. The PE2 results with RTT19 showed up to $28\% \pm 0.7\%$ editing at the target, indicating that the additional mutation in the RTT increased by 2.7-fold the desired modification at +13 (Figure 5A). The PE2 results with RTT31 also showed an increase of 1.6-fold with an editing percentage of up to $25\% \pm 0.7\%$. The PE3 results showed up to $42\% \pm 0.7\%$ modification at the target for pegRNAs with RTT19 and RTT31 (Figure 5B). We observed that the target modification at +13 was significantly influenced by the simultaneous modification of the PAM sequence and an additional mutation at different positions around the target. The distance from the target and the type of nucleotide modification seemed to play a role in that efficiency.

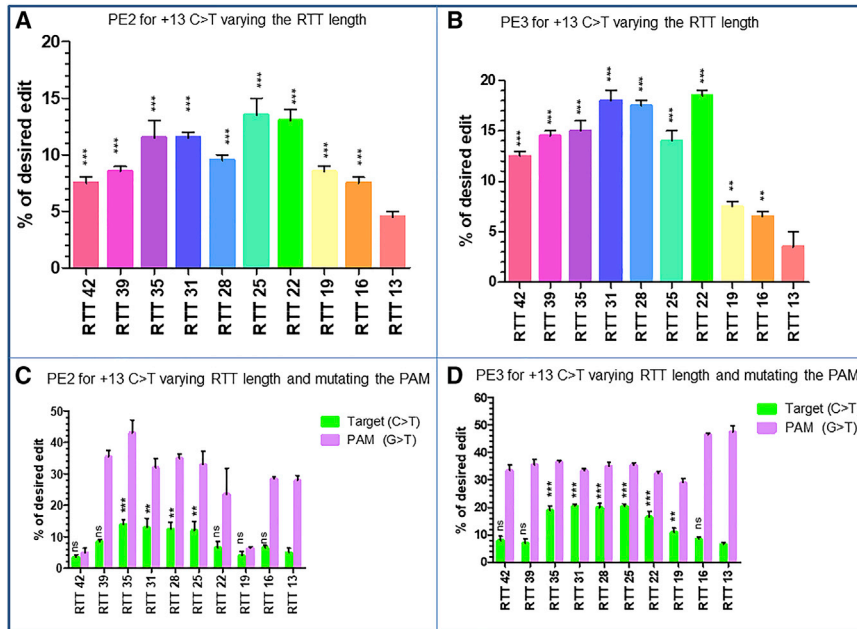


Figure 4. Influence of the RTT length on the target

(A and B) The PE2 (A) and PE3 (B) results for the introduction of c.8713C>T mutation in exon 59 of *DMD* gene when the RTT length varies from 13 (RTT 13) to 42 (RTT 42). The difference was not statistically significant (ns) either for PE2 or PE3 using the Kruskal-Wallis test. (C and D) The PE2 (C) and PE3 (D) results when the RTT length varies from RTT 13 to RTT 42. The modification at the target (green) is done simultaneously with the modification of the PAM sequence (purple). The experiments were done in triplicates ($n = 3$). The p values were calculated using the Kruskal-Wallis test. The editing percentages were compared between RTT13 and other RTTs for the mutation at the target site. *** $p = 0.001$; ** $p = 0.01$; * $p < 0.05$; ns, non-significant difference.

From the PE3 strategy, we selected harvested samples transfected with pegRNAs in which the third additional mutation could induce a synonymous mutation. The results were analyzed by Illumina deep sequencing. These included +3T>C RTT19, +9T>C RTT19, +12A>G RTT19, +15A>G RTT19, +3T>C RTT31, +9T>C RTT31, +12A>G RTT31, and +15A>G RTT31. The Illumina sequencing results were almost identical to those obtained with Sanger sequencing (Figure 5C). Deep sequencing of these amplicons showed average indels of 0.9% with a maximum of 1.5% recorded with +15A>G RTT31.

Combinations of more than two additional mutations

Since the combination of two additional mutations around the target significantly influenced its efficiency, we decided to check whether more than two mutations could give more interesting results. We designed a pegRNA (Table 1, row 1J) containing four mutations in addition to the target mutation at +13. A total of five simultaneous mutations were inserted in a single pegRNA (RTT19, PBS14) including: the target (+13C>T), the PAM (+6G>T), the third additional mutation (+2C>T), the fourth additional mutation (+10C>T), and the fifth additional mutation (+17A>T). The PE3 strategy results showed that the interactions between all these mutations decreased the editing efficiency at +13; moreover, each individual nucleotide mutation was also decreased (Figure 5D).

Checking whether the type of nucleotide can influence the modification of the target

We decided to change the C nucleotide at the +13 target to either an A, a G, or a T. We designed different pegRNAs with RTT19 to verify the potential effects on the nucleotide changes (Table 1, rows 1K). While changing the C to T at position +13, we also simultaneously changed at the position +3 either the T to C (C>T +3T>C RTT19),

T to G (C>T +3T>G RTT19), or T to A (C>T +3T>A RTT19). Similarly, we also changed the C to G and the C to A at +13, while simultaneously changing at the position +3 either the T to C (C>G +3T>C RTT19 and C>A +3T>C RTT19), T to G (C>G +3T>G RTT19 and C>A +3T>G RTT19), or T to A (C>G +3T>A RTT19 and C>A +3T>A RTT19). With the PE3 results, we observed up to $36.5\% \pm 0.5\%$, $58\% \pm 1.1\%$, and $40\% \pm 1.8\%$ editing efficiency, respectively for C to T, C to G, and C to A modification at the target (Figure 6A). This indicated that the type of nucleotide to be changed at the target and the type of nucleotides at the additional mutation sites highly influenced the editing efficiency. The same experiment was done with different pegRNAs with RTT31. The results were lower than those observed with pegRNAs with RTT19 (Figure 6B).

Correction of the C to T mutation at +13

With the collaboration of the Institut de Myologie de Paris, we obtained a human myoblast cell line carrying the c.8713C>T point mutation. For the correction of that mutation, we selected two pegRNAs (Table 1, rows 1L) from the different optimizations we made to introduce the same mutation in HEK293T cells to create a stop codon. We chose the +9T>C RTT19 and +9T>C RTT31, which both gave about 35% modification in HEK293T using the PE3 strategy. These pegRNAs permitted, while inducing the modification at the target (+13C>T), introduction of a silent mutation in the PAM sequence (+6G>T) and additional mutation (+9T>C). In these pegRNAs, we changed only the nucleotide at the target position to correct the mutation instead of creating the mutation. In addition to the PE3 strategy, which uses the pCMV-PE2 plasmid with the pegRNA and sgRNA plasmids, we also tested the PE5 strategy recently described by Chen et al.,²⁴ which uses the pCMV-PEmax-P2A-hMLH1dn with the pegRNA and sgRNA plasmids. After proliferation, 100,000 human myoblasts carrying the c.8713C>T mutation were electroporated separately with 1 μ g of each of the two selected and modified pegRNAs and 1 μ g of pCMV-PE2 plasmid for PE3 strategy or pCMV-PEmax-P2A-hMLH1dn for PE5 strategy. Three to five days

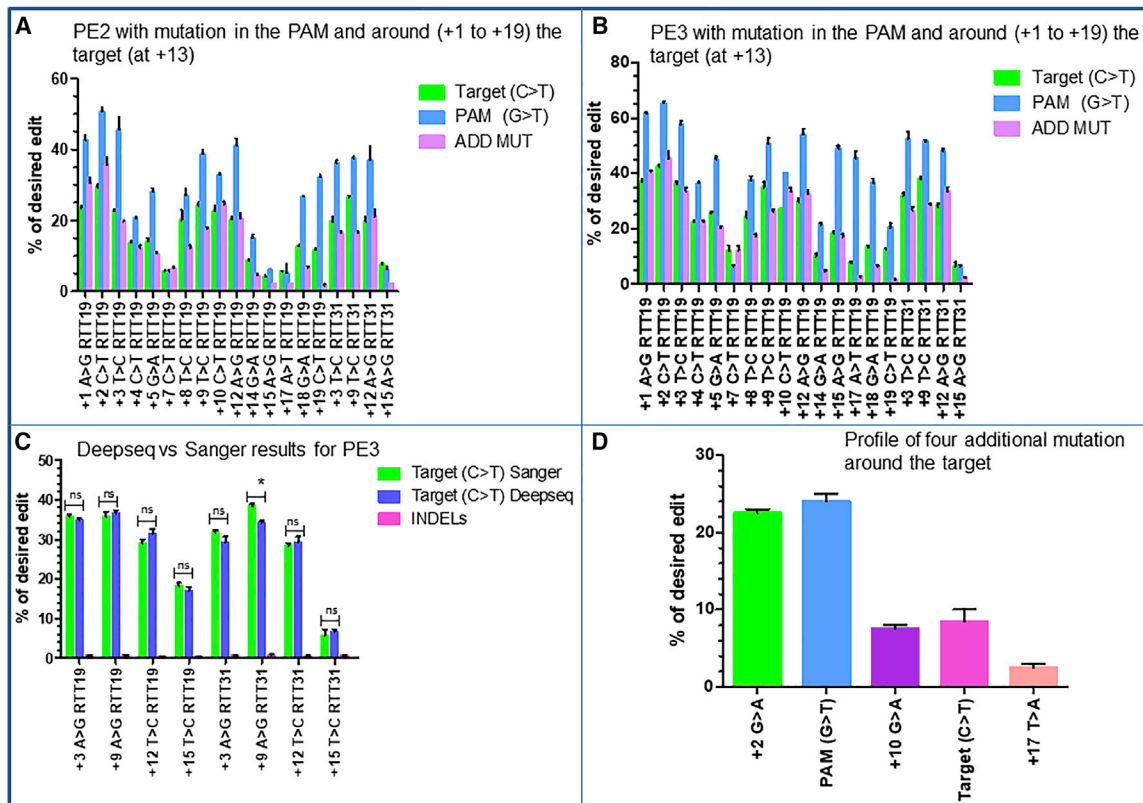


Figure 5. Influence of simultaneous additional mutations on the target

(A and B) Variations in editing efficacy for PE2 (A) and PE3 (B) strategies for the introduction of c.8713C>T mutation in exon 59 of *DMD* gene when the PAM sequence and a third additional nucleotide (ADD MUT) are simultaneously modified. The three mutations are all introduced by a pegRNA. The third mutation is introduced at different positions (from +1 to +15) in RTT19 and RTT31. (C) Illumina deep sequencing and Sanger sequencing results for PE3 strategy (shown in B) when the modification at the target is done simultaneously with the modification in the PAM sequence and the introduction of the third additional silent mutations at different positions of RTT19 and RTT31. * $p = 0.01$ using the non-parametric Mann-Whitney U test. ns, non-significant difference. (D) Individual results for the combination of five different mutations at different positions of the RTT19 sequence. The experiments were done in independent triplicates ($n = 3$).

after electroporation, cells were collected and separated into two parts. One part was immediately used for DNA extraction, PCR amplification, and sequencing through the Sanger method. The results for the PE3 strategy showed $17\% \pm 2.1\%$ and $8\% \pm 1.4\%$ editing, respectively, for the +9T>C RTT19 and +9T>C RTT31 pegRNAs (Figure 7A). The PE5 strategy showed $21\% \pm 1.4\%$ and $14\% \pm 1.4\%$ editing efficiency, respectively for the +9T>C RTT19 and +9T>C RTT31 pegRNAs (Figure 7A). These represented 1.2-fold and 1.7-fold increases, respectively with +9T>C RTT19 and +9T>C RTT31 pegRNAs using the PE5 strategy. The other part of the harvested cells for the PE5 strategy was used for myotube formation through the fusion of myoblasts to verify whether expression of the dystrophin protein was restored. Western blotting carried out with $20 \mu\text{g}$ of total protein showed dystrophin expression of 42% and 31%, respectively for the two pegRNAs (Figure 7B).

DISCUSSION

The prime editing technique for genome editing is constantly being optimized.^{23,24,31} Our results show that increasing the RTT length

for a target mutation site that is far from the nick site improved the editing efficiency. It has been demonstrated that some target sites prefer long RTT sequences while others prefer short RTT sequences.²² However, in combination with the RTT length, our results showed that the addition of one or many nucleotide modifications at different sites from the intended edit significantly improved the editing outcome. Chen et al.²⁴ also indicated that inserting 1–4 silent mutations between the positions +7 and +14 improved by 1.5-fold the edit at the position +6.

We demonstrated that the position of the target mutation, the type of nucleotide to be modified at that position, and the type and position of the additional nucleotide mutation around the desired target highly influenced the nucleotide change efficiency at the target. The mechanism by which this interaction occurs is currently poorly understood. The additional mutations around the target may play a role during the mismatch repair mechanism favoring the installation of the intended modification.²⁴ These additional mutations can interact by increasing or decreasing the editing efficiency of one or the other nucleotide. A

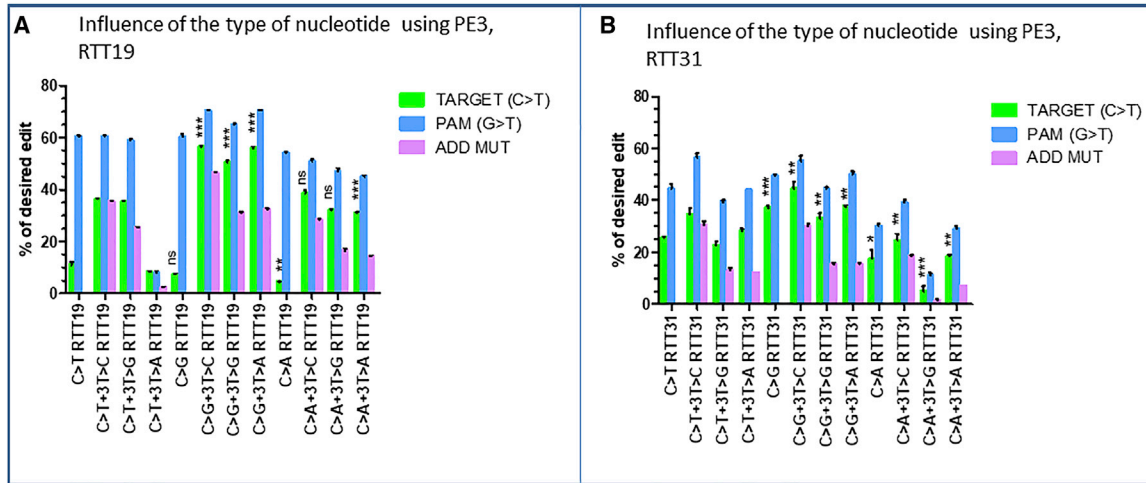


Figure 6. Influence of the type of nucleotide to be changed at the target

This figure shows the PE3 results with different pegRNAs having RTT19 (A) and RTT31 (B). Here, the C nucleotide at the target site is changed either to T (C>T), G (C>G), or A (C>A). Each time these mutations are done, the PAM sequence at the position +6 and the third additional nucleotide (ADD MUT) at the position +3 are simultaneously changed as indicated in the x axis of the graph. The experiments were done in independent triplicates (n = 3). The p values were calculated using the non-parametric Mann-Whitney U test. The C>T groups were compared with C>G and C>A groups. ***p = 0.0001, **p = 0.001, *p = 0.01, and p > 0.05 (ns) for 5% confidence interval.

negative impact on the mutation at +13 and on each additional nucleotide taken individually was observed when four additional mutations that previously individually showed high editing percentages were inserted simultaneously by the same RTT sequence. Since the mismatch repair varies by mismatch type,³² the type and the position of the additional mutation could repress or favor its installation. The distance between the nucleotide to be modified and additional mutations also plays a role during the process.

This optimized strategy by modifying the RTT sequence increased by 3.8-fold the intended modification at position +13. When the nucleotide at the target in the non-PAM strand was changed to C instead of A in our case, we observed a 6.6-fold increase using a pegRNA with only one nucleotide difference (C>G instead of C>T). This indicates that point mutation can be corrected in the *DMD* gene more effectively when taking into consideration the type of nucleotide to be changed and the possibility of inserting one or more additional silent mutations.

Combining this strategy with the PEmax-hMLH1dn strategy,²⁴ we obtained up to a 1.7-fold increase in editing efficiency for the correction of c.8713C>T mutation. The PEmax-hMLH1dn strategy permits the disruption of *hMLH1* mismatch repair gene, which acts at the genomic damage checkpoint to stabilize the MutS-DNA complex³³ and favor the installation of the intended mutation. The improvement induced by modifications of repair factors, among which MLH1 gene is the best candidate, might vary depending on cell lines and the type of edit.³⁴ This strategy permitted us to achieve 22% modification in human myoblasts for the correction of c.8713C>T mutation. This percentage represents a good modification level for the *DMD* gene. In fact, the dystrophin nuclear domain contains about 30 nuclei and is about 439 μm long.^{35–37} Considering that a muscle fiber is

made of thousands of nuclei, the correction in one nucleus in a nuclear domain (approximately 3%) could be enough for a phenotypic improvement.

MATERIALS AND METHODS

Plasmids

The pCMV-PE2, the pCMV-PEmax-P2A-hMLH1dn and pU6-pegRNA-GG-acceptor plasmids were a gift from David Liu (Addgene plasmids #132775, #174828, and #132777). Cloning in these plasmids was done as described by Anzalone et al.²² Oligonucleotides used for the construction of pegRNAs were purchased from IDT (Coralville, IA, USA).

Cell culture

HEK293T were grown in DMEM-HG medium (Wisent, Saint-Jean-Baptiste, QC, Canada) supplemented with 10% fetal bovine serum (FBS) (Wisent) and 1% penicillin-streptomycin (Wisent) at 37°C with 5% CO₂ in a humidified incubator. The day before transfection, cells were detached from the flask with a trypsin-EDTA solution (Sigma-Aldrich Canada, Oakville, ON, Canada) and counted. Detached cells were plated on a 24-well plate at a density of 60,000 cells per well with 1 mL of culture medium. On the transfection day, the medium was replaced with 500 μL of fresh medium. Cells were transfected with 1 μg of total DNA (500 ng of each plasmid when co-transfection was required) with Lipofectamine 2000 (Invitrogen, Carlsbad, CA, USA) according to the manufacturer's instructions. The medium was changed to 1 mL of fresh medium 24 h later, and cells were maintained in incubation for 72 h before genomic DNA extraction.

The human myoblasts were grown in a home-made medium made of 4 volumes of DMEM-HG medium for 1 volume of medium 199

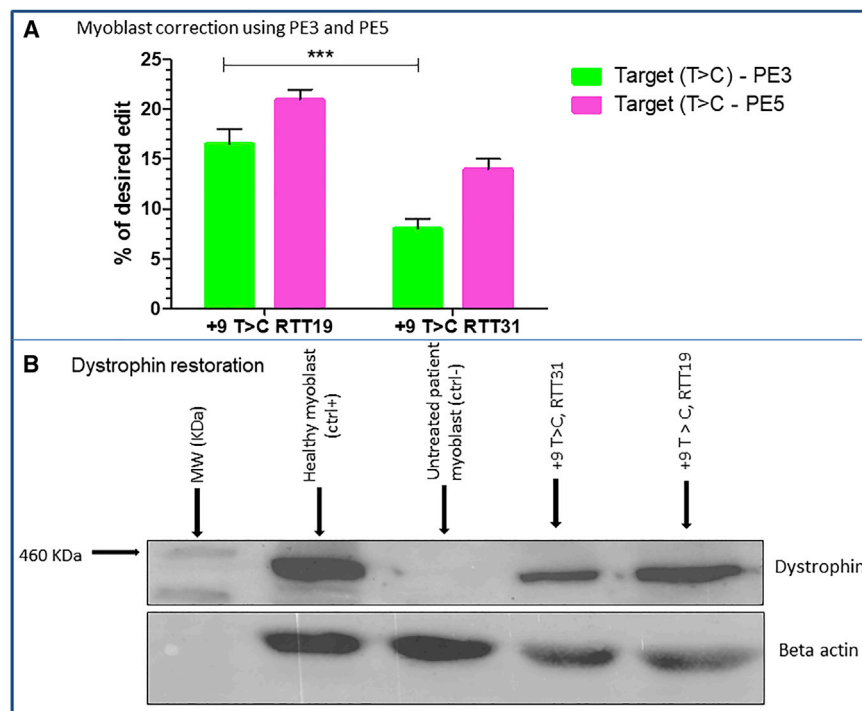


Figure 7. Correction of DMD c.8713C>T mutation

(A) Editing percentage for PE3 and PE5 strategies in human myoblasts for the correction of c.8713C>T mutation in exon 59 of *DMD* gene. The RTT19 and RTT31 used here permitted us to induce the desired modification (T>C) at +13 while modifying simultaneously the PAM sequence (G>T) at +6 and the additional nucleotide (T>C) at +9. The experiments were done in triplicates ($n = 3$). The mean editing percentage at the target site was statistically significant with ($***p < 0.001$) using the non-parametric Mann-Whitney U test. (B) Western blot resulting from 20 μ g of total protein obtained by the lysis of myotubes from the culture plate. It indicates the molecular weight marker (460 kDa), the negative control sample (Ctrl-), which used myoblasts with point mutation in exon 59, the positive controls (Ctrl+), which were healthy human myoblasts, and the samples treated with the pegRNAs described in (A).

(Invitrogen) supplemented with 25 μ g/mL fetuin (Life Technologies, Carlsbad, CA, USA), 5 ng/mL human epidermal growth factor (Life Technologies), 0.5 ng/mL basic fibroblast growth factor (Life Technologies), 5 μ g/mL insulin (Sigma-Aldrich Canada, 91077C-1G), 0.2 μ g/mL dexamethasone (Sigma-Aldrich Canada). A total of 2 μ g of plasmids (1 μ g of pCMV-PE2 or pCMV-PEmax-P2A-hMLH1dn plasmid and 1 μ g of pU6-GG-acceptor plasmid containing the pegRNA sequence and the sgRNA for PE3) were added to 100,000 human myoblasts and electroporated with the Neon Transfection System following the program 1,100 V/20 ms/2 pulses. These electroporated cells were placed in one well of a 24-well culture plate containing 500 μ L of the home-made medium. The electroporation medium was changed to 1 mL of fresh medium after 24 h, and cells were detached with trypsin and harvested in 1 mL of culture medium for the next 48 h. Half of the harvested cells was used for DNA extraction, and the remaining volume was transferred to one well of a 6-well culture plate containing 2 mL of the home-made medium. At 80%–90% confluency, the medium was changed to 2 mL of DMEM containing 1% FBS to induce myoblast fusion to form myotubes, which were harvested a few days later for western blot analysis of dystrophin.

Genomic DNA preparation, amplification, and sequencing

HEK293T cells were detached from wells directly with up-and-down pipetting of the culture medium and transferred in 1.5-mL Eppendorf tubes. Human myoblasts were detached using trypsin-EDTA solution (Sigma-Aldrich Canada) and collected in 1 mL of the original medium. HEK293T cells or human myoblasts were spun for 5 min at 9,000 rpm in a microcentrifuge at room temperature.

Cell pellets were washed once with 1 mL of 1 \times phosphate-buffered saline and spun again for 5 min at 9,000 rpm. Genomic DNA was prepared using the DirectPCR Lysis Reagent (Viagen Biotech, Los Angeles, CA, USA). In brief, 50 μ L of DirectPCR Lysis Reagent containing 0.5 μ L of a proteinase K solution (20 mg/mL) was added to each cell pellet and incubated overnight at 56°C followed by another incubation at 85°C for 45 min and centrifugation at 13,000 rpm for 5 min; 1 μ L of each genomic DNA preparation (supernatant) was used for the PCR reaction. For each primer set (Table 2), PCR temperature cycling was as follows: 98°C for 30 s and 35 cycles of 98°C for 10 s, 60°C for 20 s, and 72°C for 45 s. A final extension at 72°C for 5 min was also performed. We used Phusion High-Fidelity DNA polymerase from Thermo Fisher Scientific (Waltham, MA, USA) for all PCR reactions. Five microliters of amplicons was electrophoresed in 1 \times Tris/borate/EDTA buffer on 1% agarose gel to control the PCR reaction qualities and to make sure that only one specific band was present.

Sanger sequencing

Amplicons from PCR (i.e., the remaining 45 μ L) were sent to the sequencing platform of the CHU de Québec Research Center for Sanger sequencing. An internal primer (Table 2) was used for polymerization using the BigDye Terminator v3.1 (Thermo Fisher Scientific). Sequences were analyzed with the EditR online program (<http://baseeditr.com>)³⁸ to determine the editing percentage in the targeted region of the *DMD* gene.

Deep sequencing analysis

Deep sequencing samples were prepared by a PCR reaction (as described above) with special primers containing a barcode sequence to permit the subsequent deep sequencing (Table 2). PCR samples were sent to the Genome Québec Innovation Center at McGill University to sequence amplicons with the Illumina sequencer. Roughly

6,000–10,000 reads were obtained per sample. Illumina sequencing results were analyzed with the CRISPResso2 online program (<https://crispresso.pinellolab.partners.org/>).³⁹

Western blot analysis

Myotubes were detached directly from a culture plate with 400 μ L of lysis buffer supplemented with protease inhibitors. One microliter of extracted proteins and different concentrations of BSA (used as standard) were put onto a nitrocellulose membrane and colored with amino black 10B. The membrane was scanned by the ChemiDoc XRS+ system (Bio-Rad Laboratories, Hercules, CA, USA) and quantified using ImageLab 6.0.1 software (Bio-Rad) according to the manufacturer's instructions. Twenty micrograms of extracted protein samples was separated by SDS-PAGE (4%–7%) and transferred onto a polyvinylidene fluoride membrane. A mouse monoclonal antibody against dystrophin (clone MANDYS8; Abnova, Taipei, Taiwan) and the mouse β -actin antibody against β -actin (Thermo Fisher Scientific) were used for immunoblotting analysis. Horseradish peroxidase-conjugated goat anti-mouse (Thermo Fisher Scientific) was used as secondary antibody. The membrane was developed using Clarity Western ECL substrate (Bio-Rad) and scanned by the ChemiDoc XRS+ system (Bio-Rad).

Statistical analysis

Data were analyzed using the GraphPad PRISM 5.0 software package (Graph Pad Software, La Jolla, CA, USA). Comparisons between the mean editing percentage among different groups were performed using the Mann-Whitney non-parametric U test. Comparisons between single pegRNAs were performed using Kruskal-Wallis one way ANOVA. A p value of <0.05 was considered statistically significant for a 5% confidence interval.

DATA AVAILABILITY

The datasets generated during and/or analyzed during the current study are available from the corresponding author on reasonable request.

ACKNOWLEDGMENTS

This work was supported by grants from Jesse's Journey – the Foundation for Cell and Gene Therapy, the Canadian Institutes of Health Research (CIHR), and the TheCell network (Réseau de Thérapie Cellulaire, Tissulaire et Génique du Québec) of the Fond de Recherche du Québec en Santé (FRQS).

AUTHOR CONTRIBUTIONS

C.H.M., J.R., and J.P.T. conceived and designed the experiments. C.H.M., J.R., Y.L., A.B., K.M., and V.M. performed the experiments. J.P.T. supervised the research. C.H.M. and J.P.T. wrote the article.

DECLARATION OF INTERESTS

The authors declare no competing interests.

REFERENCES

- Polakoff, R.J., Morton, A.A., Koch, K.D., and Rios, C.M. (1998). The psychosocial and cognitive impact of Duchenne's muscular dystrophy. *Semin. Pediatr. Neurol.* 5, 116–123. [https://doi.org/10.1016/S1071-9091\(98\)80027-2](https://doi.org/10.1016/S1071-9091(98)80027-2).
- Porteous, D., Davies, B., English, C., and Atkinson, J. (2021). An Integrative review Exploring Psycho-Social impacts and therapeutic Interventions for parent Caregivers of Young People living with Duchenne's muscular dystrophy. *Children* 8, 212. <https://doi.org/10.3390/children8030212>.
- Ciafaloni, E., Kumar, A., Liu, K., Pandya, S., Westfield, C., Fox, D.J., Caspers Conway, K.M., Cunniff, C., Mathews, K., West, N., et al. (2016). Age at onset of first signs or symptoms predicts age at loss of ambulation in Duchenne and Becker Muscular Dystrophy: Data from the MD STARnet. *J. Pediatr. Rehabil. Med.* 9, 5–11. <https://doi.org/10.3233/PRM-160361>.
- Ryder, S., Leadley, R.M., Armstrong, N., Westwood, M., de Kock, S., Butt, T., Jain, M., and Kleijnen, J. (2017). The burden, epidemiology, costs and treatment for Duchenne muscular dystrophy: an evidence review. *Orphanet J. Rare Dis.* 12, 79. <https://doi.org/10.1186/s13023-017-0631-3>.
- Crisafulli, S., Sultana, J., Fontana, A., Salvo, F., Messina, S., and Trifirò, G. (2020). Global epidemiology of Duchenne muscular dystrophy: an updated systematic review and meta-analysis. *Orphanet J. Rare Dis.* 15, 141. <https://doi.org/10.1186/s13023-020-01430-8>.
- Nowak, K.J., and Davies, K.E. (2004). Duchenne muscular dystrophy and dystrophin: pathogenesis and opportunities for treatment. *EMBO Rep.* 5, 872–876. <https://doi.org/10.1038/sj.embor.7400221>.
- Gao, Q., and McNally, E.M. (2015). The Dystrophin Complex: structure, function and implications for therapy. *Compr. Physiol.* 5, 1223–1239. <https://doi.org/10.1002/cphy.c140048>.
- Piovesan, A., Caracausi, M., Antonaros, F., Pelleri, M.C., and Vitale, L. (2016). GeneBase 1.1: a tool to summarize data from NCBI gene datasets and its application to an update of human gene statistics. *Database* 2016, baw153. <https://doi.org/10.1093/database/baw153>.
- Happi Mbakam, C., Lamothe, G., Tremblay, G., and Tremblay, J.P. (2022). CRISPR-Cas9 gene therapy for Duchenne muscular dystrophy. *Neurotherapeutics*. <https://doi.org/10.1007/s13311-022-01197-9>.
- Happi Mbakam, C., Lamothe, G., and Tremblay, J.P. (2022). Therapeutic strategies for dystrophin replacement in Duchenne muscular dystrophy. *Front. Med.* 9, 859930. <https://doi.org/10.3389/fmed.2022.859930>.
- Bladen, C.L., Salgado, D., Monges, S., Foncuberta, M.E., Kekou, K., Kosma, K., Dawkins, H., Lamont, L., Roy, A.J., Chamova, T., et al. (2015). The TREAT-NMD DMD Global Database: analysis of more than 7,000 Duchenne muscular dystrophy mutations. *Hum. Mutat.* 36, 395–402. <https://doi.org/10.1002/humu.22758>.
- Iyombe-Engembe, J.-P., Ouellet, D.L., Barbeau, X., Rousseau, J., Chapdelaine, P., Lagüe, P., and Tremblay, J.P. (2016). Efficient Restoration of the dystrophin gene reading Frame and protein structure in DMD myoblasts using the CinDel method. *Mol. Ther.* 16.
- Duchêne, B.L., Cherif, K., Iyombe-Engembe, J.-P., Guyon, A., Rousseau, J., Ouellet, D.L., Barbeau, X., Lagüe, P., and Tremblay, J.P. (2018). CRISPR-induced deletion with SaCas9 restores dystrophin expression in dystrophic models in Vitro and in vivo. *Mol. Ther.* 26, 2604–2616. <https://doi.org/10.1016/j.ymthe.2018.08.010>.
- Chemello, F., Chai, A.C., Li, H., Rodriguez-Caycedo, C., Sanchez-Ortiz, E., Atmanli, A., Mireault, A.A., Liu, N., Bassel-Duby, R., and Olson, E.N. (2021). Precise correction of Duchenne muscular dystrophy exon deletion mutations by base and prime editing. *Sci. Adv.* 7, eabg4910. <https://doi.org/10.1126/sciadv.abg4910>.
- Xiang, X., Zhao, X., Pan, X., Dong, Z., Yu, J., Li, S., Liang, X., Han, P., Qu, K., Jensen, J.B., et al. (2021). Efficient correction of Duchenne muscular dystrophy mutations by SpCas9 and dual gRNAs. *Mol. Ther. Nucleic Acids* 24, 403–415. <https://doi.org/10.1016/j.omtn.2021.03.005>.
- Min, Y.-L., Li, H., Rodriguez-Caycedo, C., Mireault, A.A., Huang, J., Shelton, J.M., McAnally, J.R., Amoasii, L., Mammen, P.P.A., Bassel-Duby, R., et al. (2019). CRISPR-Cas9 corrects Duchenne muscular dystrophy exon 44 deletion mutations in mice and human cells. *Sci. Adv.* 5, eaav4324. <https://doi.org/10.1126/sciadv.aav4324>.

17. Koo, T., Lu-Nguyen, N.B., Malerba, A., Kim, E., Kim, D., Cappellari, O., Cho, H.-Y., Dickson, G., Popplewell, L., and Kim, J.-S. (2018). Functional Rescue of dystrophin Deficiency in mice caused by Frameshift mutations using *Campylobacter jejuni* Cas9. *Mol. Ther.* 26, 1529–1538. <https://doi.org/10.1016/j.ymthe.2018.03.018>.
18. Xu, L., Zhang, C., Li, H., Wang, P., Gao, Y., Mokadam, N.A., Ma, J., Arnold, W.D., and Han, R. (2021). Efficient precise in vivo base editing in adult dystrophic mice. *Nat. Commun.* 12, 3719. <https://doi.org/10.1038/s41467-021-23996-y>.
19. Happi Mbakam, C., Rousseau, J., Tremblay, G., Yameogo, P., and Tremblay, J.P. (2022). Prime editing permits the introduction of specific mutations in the gene Responsible for Duchenne muscular dystrophy. *Int. J. Mol. Sci.* 23, 6160. <https://doi.org/10.3390/ijms23116160>.
20. Hille, F., and Charpentier, E. (2016). CRISPR-Cas: biology, mechanisms and relevance. *Phil. Trans. Biol. Sci.* 371, 20150496. <https://doi.org/10.1098/rstb.2015.0496>.
21. López, S.M., Balog-Alvarez, C., Vitha, S., Bettis, A.K., Canessa, E.H., Kornegay, J.N., and Nghiem, P.P. (2020). Challenges associated with homologous directed repair using CRISPR-Cas9 and TALEN to edit the DMD genetic mutation in canine Duchenne muscular dystrophy. *PLoS One* 15, e0228072. <https://doi.org/10.1371/journal.pone.0228072>.
22. Anzalone, A.V., Randolph, P.B., Davis, J.R., Sousa, A.A., Koblan, L.W., Levy, J.M., Chen, P.J., Wilson, C., Newby, G.A., Raguram, A., et al. (2019). Search-and-replace genome editing without double-strand breaks or donor DNA. *Nature* 576, 149–157. <https://doi.org/10.1038/s41586-019-1711-4>.
23. Nelson, J.W., Randolph, P.B., Shen, S.P., Everette, K.A., Chen, P.J., Anzalone, A.V., An, M., Newby, G.A., Chen, J.C., Hsu, A., et al. (2021). Engineered pegRNAs improve prime editing efficiency. *Nat. Biotechnol.* 1–9. <https://doi.org/10.1038/s41587-021-01039-7>.
24. Chen, P.J., Hussmann, J.A., Yan, J., Knipping, F., Ravisankar, P., Chen, P.-F., Chen, C., Nelson, J.W., Newby, G.A., Sahin, M., et al. (2021). Enhanced prime editing systems by manipulating cellular determinants of editing outcomes. *Cell* 184, 5635–5652. e29. <https://doi.org/10.1016/j.cell.2021.09.018>.
25. Choi, J., Chen, W., Suiter, C.C., Lee, C., Chardon, F.M., Yang, W., Leith, A., Daza, R.M., Martin, B., and Shendure, J. (2021). Precise genomic deletions using paired prime editing. *Nat. Biotechnol.* 1–9. <https://doi.org/10.1038/s41587-021-01025-z>.
26. Anzalone, A.V., Gao, X.D., Podracky, C.J., Nelson, A.T., Koblan, L.W., Raguram, A., Levy, J.M., Mercer, J.A.M., and Liu, D.R. (2021). Programmable deletion, replacement, integration and inversion of large DNA sequences with twin prime editing. *Nat. Biotechnol.* 1–10. <https://doi.org/10.1038/s41587-021-01133-w>.
27. Rousseau, J., Mbakam, C.H., Guyon, A., Tremblay, G., Begin, F.G., and Tremblay, J.P. (2020). Specific mutations in genes responsible for alzheimer and for duchenne muscular dystrophy introduced by base editing and PRIME editing. Preprint at bioRxiv. <https://doi.org/10.1101/2020.07.31.230565>.
28. Kim, N., Kim, H.K., Lee, S., Seo, J.H., Choi, J.W., Park, J., Min, S., Yoon, S., Cho, S.-R., and Kim, H.H. (2020). Prediction of the sequence-specific cleavage activity of Cas9 variants. *Nat. Biotechnol.* 38, 1328–1336. <https://doi.org/10.1038/s41587-020-0537-9>.
29. Walton, R.T., Christie, K.A., Whittaker, M.N., and Kleinstiver, B.P. (2020). Unconstrained genome targeting with near-PAMless engineered CRISPR-Cas9 variants. *Science* 368, 290–296. <https://doi.org/10.1126/science.aba8853>.
30. Kweon, J., Yoon, J.-K., Jang, A.-H., Shin, H.R., See, J.-E., Jang, G., Kim, J.-I., and Kim, Y. (2021). Engineered prime editors with PAM flexibility. *Mol. Ther.* 29, 2001–2007. <https://doi.org/10.1016/j.ymthe.2021.02.022>.
31. Liu, P., Liang, S.-Q., Zheng, C., Mintzer, E., Zhao, Y.G., Ponnieselvan, K., Mir, A., Sontheimer, E.J., Gao, G., Flotte, T.R., et al. (2021). Improved prime editors enable pathogenic allele correction and cancer modelling in adult mice. *Nat. Commun.* 12, 2121. <https://doi.org/10.1038/s41467-021-22295-w>.
32. Lujan, S.A., Clausen, A.R., Clark, A.B., MacAlpine, H.K., MacAlpine, D.M., Malc, E.P., Mieczkowski, P.A., Burkholder, A.B., Fargo, D.C., Gordenin, D.A., et al. (2014). Heterogeneous polymerase fidelity and mismatch repair bias genome variation and composition. *Genome Res.* 24, 1751–1764. <https://doi.org/10.1101/gr.178335.114>.
33. Wu, Q., and Vasquez, K.M. (2008). Human MLH1 protein Participates in genomic damage Checkpoint Signaling in Response to DNA Interstrand Crosslinks, while MSH2 Functions in DNA repair. *PLoS Genet.* 4, e1000189. <https://doi.org/10.1371/journal.pgen.1000189>.
34. Ferreira da Silva, J., Oliveira, G.P., Arasa-Verge, E.A., Kagiou, C., Moretton, A., Timelthaler, G., Jiricny, J., and Loizou, J.I. (2022). Prime editing efficiency and fidelity are enhanced in the absence of mismatch repair. *Nat. Commun.* 13, 760. <https://doi.org/10.1038/s41467-022-28442-1>.
35. Blau, H.M., Pavlath, G.K., Rich, K., and Webster, S.G. (1990). Localization of muscle gene products in nuclear domains: does this constitute a problem for myoblast therapy? *Adv. Exp. Med. Biol.* 280, 167–172. https://doi.org/10.1007/978-1-4684-5865-7_19.
36. Kinoshita, I., Vilquin, J.T., Asselin, I., Chamberlain, J., and Tremblay, J.P. (1998). Transplantation of myoblasts from a transgenic mouse overexpressing dystrophin produced only a relatively small increase of dystrophin-positive membrane. *Muscle Nerve* 21, 91–103. [https://doi.org/10.1002/\(sici\)1097-4598](https://doi.org/10.1002/(sici)1097-4598).
37. Bruusgaard, J.C., Liestøl, K., Ekmark, M., Kollstad, K., and Gundersen, K. (2003). Number and spatial distribution of nuclei in the muscle fibres of normal mice studied in vivo. *J. Physiol.* 551, 467–478. <https://doi.org/10.1113/jphysiol.2003.045328>.
38. Kluesner, M.G., Nedveck, D.A., Lahr, W.S., Garbe, J.R., Abrahante, J.E., Webber, B.R., and Moriarity, B.S. (2018). EditR: a method to quantify base editing from Sanger sequencing. *The CRISPR Journal* 1, 239–250. <https://doi.org/10.1089/crispr.2018.0014>.
39. Clement, K., Rees, H., Canver, M.C., Gehrke, J.M., Farouni, R., Hsu, J.Y., Cole, M.A., Liu, D.R., Joung, J.K., Bauer, D.E., et al. (2019). CRISPResso2 provides accurate and rapid genome editing sequence analysis. *Nat. Biotechnol.* 37, 224–226. <https://doi.org/10.1038/s41587-019-0032-3>.